ENGINEERING MECHANICS 2009
National Conference with International Participation
Svratka, Czech Republic, May 11 – 14, 2009

pp. 523–531
Paper **#228**

APPLICATION OF DIMENSION REDUCTION IN TUNNEL EXCAVATION PROBLEM

T. Janda, M. Šejnoha [1]

Summary: *The paper suggests and innovative approach to modeling of the progress of tunnel excavation. The proposed method uses dimension reduction to incorporate the supporting effect of the material in the front of and behind the examined cross section. This allows to take the advantages of the efficiency and simplicity of finite element modeling with two dimensional mesh while considering the longitudinal properties such as the width of the excavated segment. The out of plane phenomenons are calibrated via in situ measurements of convergence curves in front of and behind the tunnel heading. The dimension reduction approach can serve as an alternative to often employed convergence confinement method.*

1. Introduction

Although the process of successive excavation of tunnel tube is clearly an three dimensional problem the practical engineer often tends to employ some simplified approach. A higher time demand and the complexity of the model often force many design engineers to use the 3D analysis only for specific problems such as tunnel junctions while the linear parts of tunnel tubes analyze in 2D software.

The most common way to model the effect of excavation in two dimensions is so called convergence confinement method also known as lambda method or beta method. The principle behind this procedure lies in the devision of the excavation forces. First portion of the load due to the excavation is applied to the profile without lining simulating the state just after segment excavation with substantial supporting effect of the longitudinal vault. The remaining portion of the excavation forces are applied in the profile with lining representing the state when the tunnel heading has already moved forward and no longitudinal support takes place any more.

This paper provides a theoretical framework to how toderive the supporting effect of the longitudinal vault from in situ measurements without actually solving 3D problem.

2. Computation stages of successive excavation

The core of the proposed analysis is to examine the impact which is caused by excavation of an tunnel segment of defined width. However, this computation stage is preceded by another two stages which create the proper initial stress state. In the first stage the geostatic stresses

[1] Ing. Tomáš Janda, Ph.D., Prof. Michal Šejnoha, Ph.D., Katedra Mechaniky, Fakulta Stavební, České Vysoké Učení v Praze, Thákurova 7, 166 29 Praha 6, Tel. +420 2 2435 4498, Email. tomas.janda@fsv.cvut.cz

are computed by loading the system with self weight. No excavation is assumed in this stage allowing to adopt plane strain conditions. A three node triangular plane strain element was chosen for this type of analysis.

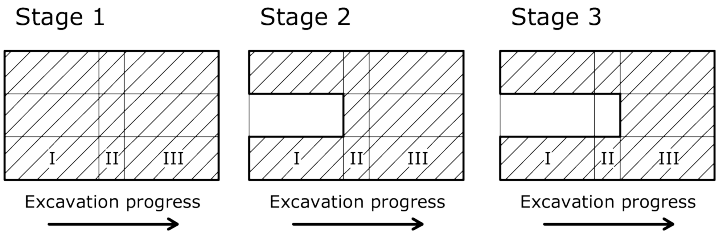

Figure 1. Computation stages and distribution of material

The second stage models the initial stress state before the actual segment excavation. The loading in the second analysis is derived from the excavation forces found along the semi-infinite tunnel tube while the element stiffness matrix takes the contribution of elements I, II and III into account for elements outside the tunnel profile, resp the contribution of elements II and III for element in the profile. Figure 1 demonstrates the arrangement of material in individual stages.

The third stage simulates the excavation of the single segment. The excavation forces are derived from the segment width and preceding stress state while the stiffness matrix belonging to the elements in the tunnel profile incorporates the supporting effect of segment III only. However the stiffness of the elements outside the profile remains unchanged and incorporates all three parts.

3. Formulation of finite element

Before formulating the detailed finite element procedures for each individual computation stage it is useful to introduce basic properties of the newly created element.

In the formulation we assume no longitudinal displacements ($w = 0$) and therefore the desired field of displacements $\boldsymbol{u}(\boldsymbol{x})$ reduces to

$$\boldsymbol{u}(\boldsymbol{x}) = \{u, v\}^T. \tag{1}$$

For linear triangular element the vector of nodal displacements $\boldsymbol{r}$ takes the form

$$\boldsymbol{r} = \{u_1, v_1, u_2, v_2, u_3, v_3\}^T. \tag{2}$$

Strain and stress components are stored in standard column vectors $\boldsymbol{\varepsilon}$ and $\boldsymbol{\sigma}$ which write

$$\boldsymbol{\varepsilon} = \{\varepsilon_{xx}, \varepsilon_{yy}, \varepsilon_{zz}, \gamma_{yz}, \gamma_{xz}, \gamma_{xy}\}^T, \tag{3}$$

$$\boldsymbol{\sigma} = \{\sigma_{xx}, \sigma_{yy}, \sigma_{zz}, \tau_{yz}, \tau_{xz}, \tau_{xy}\}^T. \tag{4}$$

Shape functions interpolates the increment of displacements at any point of the element, i.e. even outside the solved section. The interpolation in the plane of the triangular element takes advantage of the classical isoparametric formulation while the interpolation in the longitudinal

direction (outside the solved section) depends on function $f(z)$. Combining the out-of-plane and in-plane interpolation we arrive at matrix $\boldsymbol{N}$ i form

$$\boldsymbol{N}(\boldsymbol{x}) = f\left[\begin{array}{cc|cc|cc} N_1 & 0 & N_2 & 0 & N_3 & 0 \\ 0 & N_1 & 0 & N_2 & 0 & N_3 \end{array}\right], \tag{5}$$

where $N_1 = N_1(x,y)$, $N_2 = N_2(x,y)$, $N_3 = N_3(x,y)$ depend on the position in xy-plane while $f = f(z)$ is based on site measurement.

By differentiating the above matrix we receive matrix $\boldsymbol{B}$ in the form

$$\boldsymbol{B}(\boldsymbol{x}) = \left[\begin{array}{cc|cc|cc} f(z)\dfrac{\partial N_1}{\partial x} & 0 & f(z)\dfrac{\partial N_2}{\partial x} & 0 & f(z)\dfrac{\partial N_3}{\partial x} & 0 \\ 0 & f(z)\dfrac{\partial N_1}{\partial y} & 0 & f(z)\dfrac{\partial N_2}{\partial y} & 0 & f(z)\dfrac{\partial N_3}{\partial y} \\ 0 & 0 & 0 & 0 & 0 & 0 \\ \hline 0 & \dfrac{\partial f(z)}{\partial z}N_1 & 0 & \dfrac{\partial f(z)}{\partial z}N_2 & 0 & \dfrac{\partial f(z)}{\partial z}N_3 \\ \dfrac{\partial f(z)}{\partial z}N_1 & 0 & \dfrac{\partial f(z)}{\partial z}N_2 & 0 & \dfrac{\partial f(z)}{\partial z}N_3 & 0 \\ f(z)\dfrac{\partial N_1}{\partial y} & f(z)\dfrac{\partial N_1}{\partial x} & f(z)\dfrac{\partial N_2}{\partial y} & f(z)\dfrac{\partial N_2}{\partial x} & f(z)\dfrac{\partial N_3}{\partial y} & f(z)\dfrac{\partial N_3}{\partial x} \end{array}\right], \tag{6}$$

which can be decomposed into two independent matrices

$$\boldsymbol{B}(\boldsymbol{x}) = \boldsymbol{B}_z(z)\boldsymbol{B}_{x,y}(x,y), \tag{7}$$

where

$$\boldsymbol{B}_z(z) = \left[\begin{array}{ccc|ccc} f(z) & 0 & 0 & 0 & 0 & 0 \\ 0 & f(z) & 0 & 0 & 0 & 0 \\ 0 & 0 & f(z) & 0 & 0 & 0 \\ \hline 0 & 0 & 0 & \dfrac{\partial f(z)}{\partial z} & 0 & 0 \\ 0 & 0 & 0 & 0 & \dfrac{\partial f(z)}{\partial z} & 0 \\ 0 & 0 & 0 & 0 & 0 & f(z) \end{array}\right] \tag{8}$$

$$\boldsymbol{B}_{x,y}(x,y) = \left[\begin{array}{cc|cc|cc} \dfrac{\partial N_1}{\partial x} & 0 & \dfrac{\partial N_2}{\partial x} & 0 & \dfrac{\partial N_3}{\partial x} & 0 \\ 0 & \dfrac{\partial N_1}{\partial y} & 0 & \dfrac{\partial N_2}{\partial y} & 0 & \dfrac{\partial N_3}{\partial y} \\ 0 & 0 & 0 & 0 & 0 & 0 \\ \hline 0 & N_1 & 0 & N_2 & 0 & N_3 \\ N_1 & 0 & N_2 & 0 & N_3 & 0 \\ \dfrac{\partial N_1}{\partial y} & \dfrac{\partial N_1}{\partial x} & \dfrac{\partial N_2}{\partial y} & \dfrac{\partial N_2}{\partial x} & \dfrac{\partial N_3}{\partial y} & \dfrac{\partial N_3}{\partial x} \end{array}\right] \tag{9}$$

Element stiffness matrix $\boldsymbol{K}$ has to incorporate both the in-plane and out-of-plane contributions

$$\boldsymbol{K} = \int_V \boldsymbol{B}(\boldsymbol{x})^T \boldsymbol{D}\boldsymbol{B}(\boldsymbol{x})\, d\boldsymbol{x} \tag{10}$$

$$= \int_V \boldsymbol{B}_{x,y}^T(x,y)\boldsymbol{B}_z^T(z)\boldsymbol{D}\boldsymbol{B}_z(z)\boldsymbol{B}_{x,y}(x,y)\, d\boldsymbol{x} \tag{11}$$

Due to the special properties of matrices $\boldsymbol{B}_z$ and $\boldsymbol{D}$ we can rewrite the above equation

$$\boldsymbol{K} = \int_V \boldsymbol{B}_{x,y}^T(x,y)\boldsymbol{B}_z^T(z)\boldsymbol{B}_z(z)\boldsymbol{D}\boldsymbol{B}_{x,y}(x,y)\,d\boldsymbol{x} \tag{12}$$

$$= \int_A \boldsymbol{B}_{x,y}^T(x,y)\overbrace{\int_{z_1}^{z_2}\boldsymbol{B}_z^T(z)\boldsymbol{B}_z(z)\,dz}^{\boldsymbol{K}_z}\boldsymbol{D}\boldsymbol{B}_{x,y}(x,y)\,dx\,dy \tag{13}$$

$$= \int_A \boldsymbol{B}_{x,y}^T(x,y)\overbrace{\boldsymbol{K}_z\boldsymbol{D}}^{\overline{\boldsymbol{D}}}\boldsymbol{B}_{x,y}(x,y)\,dx\,dy \tag{14}$$

$$= \int_A \boldsymbol{B}_{x,y}^T(x,y)\overline{\boldsymbol{D}}\boldsymbol{B}_{x,y}(x,y)\,dx\,dy \tag{15}$$

This formulation allows for standard in-plane integration using Gaussian quadrature on the isoparametric triangular element while the out-of-plane contribution is incorporated in the matrix $\overline{\boldsymbol{D}}$. Without choosing particular form of the function $f(z)$ we can write the product $\boldsymbol{B}_z^T\boldsymbol{B}_z$ as follows

$$\boldsymbol{B}_z^T(z)\boldsymbol{B}_z(z) = \left[\begin{array}{ccc|ccc} f^2(z) & 0 & 0 & 0 & 0 & 0 \\ 0 & f^2(z) & 0 & 0 & 0 & 0 \\ 0 & 0 & f^2(z) & 0 & 0 & 0 \\ \hline 0 & 0 & 0 & \left(\dfrac{\partial f(z)}{\partial z}\right)^2 & 0 & 0 \\ 0 & 0 & 0 & 0 & \left(\dfrac{\partial f(z)}{\partial z}\right)^2 & 0 \\ 0 & 0 & 0 & 0 & 0 & f^2(z) \end{array}\right] \tag{16}$$

and performing integration we get

$$\boldsymbol{K}_z = \int_{z_1}^{z_2}\boldsymbol{B}_z^T\boldsymbol{B}_z\,dz = \left[\begin{array}{ccc|ccc} I_1 & 0 & 0 & 0 & 0 & 0 \\ 0 & I_1 & 0 & 0 & 0 & 0 \\ 0 & 0 & I_1 & 0 & 0 & 0 \\ \hline 0 & 0 & 0 & I_2 & 0 & 0 \\ 0 & 0 & 0 & 0 & I_2 & 0 \\ 0 & 0 & 0 & 0 & 0 & I_1 \end{array}\right] \tag{17}$$

where symbols I_1 and I_2 denotes definite integrals

$$I_1 = \int_{z_1}^{z_2} f^2(z)\,dz \tag{18}$$

$$I_2 = \int_{z_1}^{z_2}\left(\frac{\partial f(z)}{\partial z}\right)^2 dz \tag{19}$$

Finally recall the 3D form of material stiffness matrix $\boldsymbol{D}$ used in the above expressions

$$\boldsymbol{D} = \frac{E}{(1+\nu)(1-2\nu)}\begin{bmatrix} 1-\nu & \nu & \nu & 0 & 0 & 0 \\ \nu & 1-\nu & \nu & 0 & 0 & 0 \\ \nu & \nu & 1-\nu & 0 & 0 & 0 \\ 0 & 0 & 0 & \frac{1-2\nu}{2} & 0 & 0 \\ 0 & 0 & 0 & 0 & \frac{1-2\nu}{2} & 0 \\ 0 & 0 & 0 & 0 & 0 & \frac{1-2\nu}{2} \end{bmatrix} \tag{20}$$

4. Interpolation of convergence curves

The measured convergence curve shown in Figure 2 can be approximated with sufficient accuracy with two smoothly connected exponential functions. Assuming that the material properties of the soil body does not change significantly in the direction of the tunnel axis the convergence curve does not change its shape but simply moves forward together with advancing excavations. This allows to create function $f(z)$ which interpolates the increments of displacements outside the solved cross section.

$$f(z) = e^{\alpha_1(z+\frac{b}{2})}, z \in \left\langle -\infty, -\frac{b}{2} \right\rangle \tag{21}$$

$$f(z) = 1, z \in \left\langle -\frac{b}{2}, \frac{b}{2} \right\rangle \tag{22}$$

$$f(z) = e^{-\alpha_2(z-\frac{b}{2})}, z \in \left\langle \frac{b}{2}, \infty \right\rangle \tag{23}$$

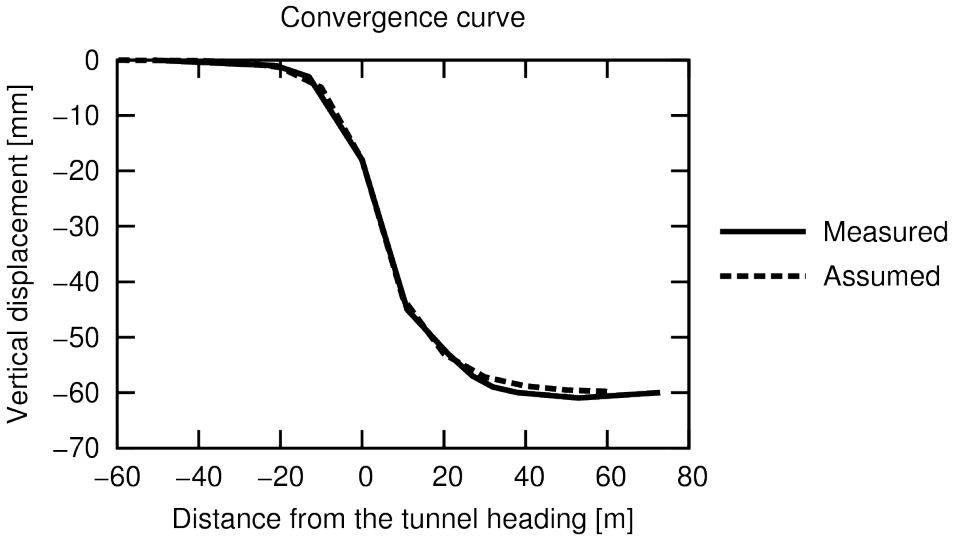

Figure 2. Convergence curve - Dependence of vertical settlement on the progress of tunnel heading

The formulation ensures that influence of the excavation decline with the distance from the examined section. For such a choice the integrals I_1 and I_2 become

$$I_1 = \frac{1}{2\alpha_1} + b + \frac{1}{2\alpha_2} \tag{24}$$

$$I_2 = \frac{\alpha_1 + \alpha_2}{2} \tag{25}$$

Similar technique is used to derive the values of excavation forces. Removing the supporting material generally restults in nodal forces given by equation

$$\boldsymbol{R} = \int_V \boldsymbol{B}^T \boldsymbol{\sigma} \, \mathrm{d}V + \int_V \boldsymbol{N}^T \boldsymbol{\gamma} \, \mathrm{d}V \tag{26}$$

where γ represents the volumetric weight and the volume V corresponds to the excavated soil. Dividing the matrices into out=of-plane and in-plane parts we can rewrite the above expression to the form

$$\boldsymbol{R} = \int_{z_3}^{z_4} \boldsymbol{B}_z^T \,\mathrm{d}z \int_A \boldsymbol{B}_{xy}^T \boldsymbol{\sigma} \,\mathrm{d}A + \int_{z_3}^{z_4} \boldsymbol{N}_z^T \,\mathrm{d}z \int_A \boldsymbol{N}_{xy}^T \boldsymbol{\gamma} \,\mathrm{d}A \tag{27}$$

where

$$\int_{z_3}^{z_4} \boldsymbol{B}_z \,\mathrm{d}z = \left[\begin{array}{ccc|ccc} I_3 & 0 & 0 & 0 & 0 & 0 \\ 0 & I_3 & 0 & 0 & 0 & 0 \\ 0 & 0 & I_3 & 0 & 0 & 0 \\ \hline 0 & 0 & 0 & I_4 & 0 & 0 \\ 0 & 0 & 0 & 0 & I_4 & 0 \\ 0 & 0 & 0 & 0 & 0 & I_3 \end{array}\right] \tag{28}$$

The values of the integrals take different values depending on the stage and the position of the element. See Table 1 for details. The different values are given by different limits of integration in each individual computation stage.

Table 1. Values of integrals used to incorporate out-of-plane stiffness

Computation stage	Element position	I_1	I_2	
2nd	Outside the profile	$\frac{1}{2\alpha_1} + b + \frac{1}{2\alpha_2}$	$\frac{\alpha_1+\alpha_2}{2}$	1m
2nd	Inside th profile	$\frac{1}{2\alpha_1} + b$	$\frac{\alpha_1}{2}$	1m
3rd	Outside the profile	$\frac{1}{2\alpha_1} + b + \frac{1}{2\alpha_2}$	$\frac{\alpha_1+\alpha_2}{2}$	1m
3rd	Inside the profile	$\frac{1}{2\alpha_1}$	$\frac{\alpha_1}{2}$	1m

The integrals I_3 and I_4 also changes with the type of computation stage and are defined in Table 2. In the second stage the integrals define the nodal load forces resulting from all past excavation while in the third stage the integrals define the excavation forces found over the single segment of finite width b.

Table 2. Values of integrals used to incorporate out-of-plane excavation forces

Computation stage	I_3	I_4
2nd	$\frac{1}{\alpha_1}$	1
3rd	1	0

5. Incremental solution in the context of continuous tunnel driving

As outlined in the previous sections the values of displacement outside the solved 2D section are interpolated using function $f(z)$ as shown in Figure 3.

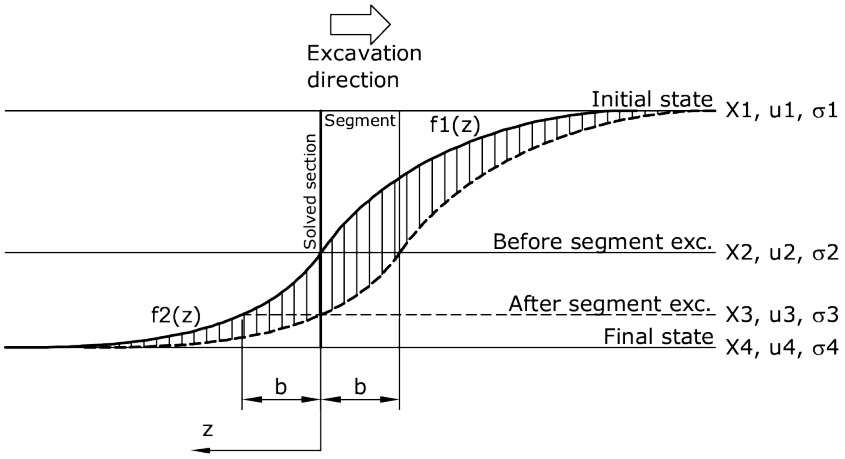

Figure 3. Properties of function $f(z)$

At the beginning of the analysis all quantities are known throughout the soil body. For instance, the values of displacement are set to zero in the initial state and the initial stress corresponds to the geostatic stress. This initial state is denoted by index 1 in Figure 3.

As the tunnel driving proceeds the soil body passes several additional states. These include

- State before single segment excavation
- State after single segment excavation
- Final state - whole length of the tunnel excavated

and are labeled with indexes 2, 3 and 4 respectively in Figure 3.

Recal that the suggested approach uses function $f(z)$ to model the distribution of the quantities along the z axis and that this function is composed of two exponential functions.

$$f(z) = f_1(z) \quad \text{for} z \leq 0 \tag{29}$$
$$= f_2(z) \quad \text{for} z \geq 0 \tag{30}$$

where function $f_1(z)$ characterizes the values in front of tunnel heading while $f_2(z)$ describes the values in the half-space which already include the tunnel tube.

If the function $f(z)$ describes certain quantity X it should satisfy the following conditions

$$f(z \to -\infty) = X_1 \tag{31}$$
$$f(z = 0) = X_2 \tag{32}$$
$$f(z \to \infty) = X_4 \tag{33}$$

which help us to write the actual functions $f_1(z)$ and $f_2(z)$ in the forms

$$f_1(z) = X_1(1 - e^{\alpha_1 z}) + X_2 e^{\alpha_1 z} \tag{34}$$
$$f_2(z) = X_4(1 - e^{-\alpha_2 z}) + X_2 e^{-\alpha_2 z} \tag{35}$$

The derivatives with respect to z are

$$f_1'(z) = (X_2 - X_1)\alpha_1 e^{\alpha_1 z} \tag{36}$$
$$f_2'(z) = (X_4 - X_2)\alpha_2 e^{-\alpha_2 z} \tag{37}$$

The assumption that the function $f(z)$ is smooth in the point $z = 0$ written as

$$f_1'(z = 0) \quad = \quad f_2'(z = 0) \tag{38}$$

provides us with relation

$$(\alpha_1 + \alpha_2)X_2 \quad = \quad \alpha_1 X_1 + \alpha_2 X_4 \tag{39}$$

When the excavation moves forward by b meters from the solved section, i.e. a single segment is excavated, the value X_2 changes to X_3. Equation (35) illuminate that the resulting value follows

$$X_3 \quad = \quad f(b) = X_4(1 - e^{-\alpha_2 b}) + X_2 e^{-\alpha_2 b} \tag{40}$$

These general property of interpolation function $f(z)$ is applied to values of stresses in the following way: the three computation stages give the stress fields denoted here as σ_1, σ_2 and σ_3 respectively. The inaccuracy of σ_2 lies in the fact that in the second stage we try to reflect all past excavation in one step. With the help of the equation derived above we rewrite the equation (40) in terms of stress and performing some basic manipulation we get

$$\sigma_4 \quad = \quad \frac{\sigma_3 - \sigma_2 e^{-\alpha_2 b}}{1 - e^{-\alpha_2 b}} \tag{41}$$

which is the approximation of the final stress state. Further rewriting and manipulating equation (39) we arrive at equation

$$\sigma_2 \quad = \quad \frac{\alpha_1 \sigma_1 + \alpha_2 \sigma_4}{\alpha_1 + \alpha_2} \tag{42}$$

which refine the initial condition for the crucial computations in stage 3.

6. Results

One cross section of the city road tunnel Blanka in Prague served as simple problem to test the method. For simplicity only the elastic material properties were assumed and no beams simulating the lining were introduced to the model during excavation stages. Figure 4 shows the differences in the vertical stress distribution before and after third computation stage which corresponds to the excavation of single soil segment.

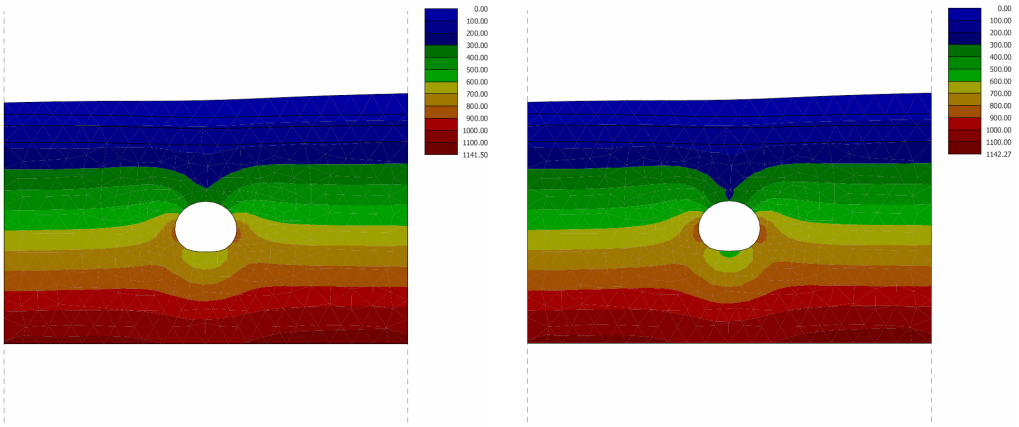

(a) (b)

Figure 4. Vertical stresses before and after the excavation single segment

Similarly, Figure 5 provides the overall vertical displacements before the segment excavation and the increment of vertical displacement caused by the segment excavation.

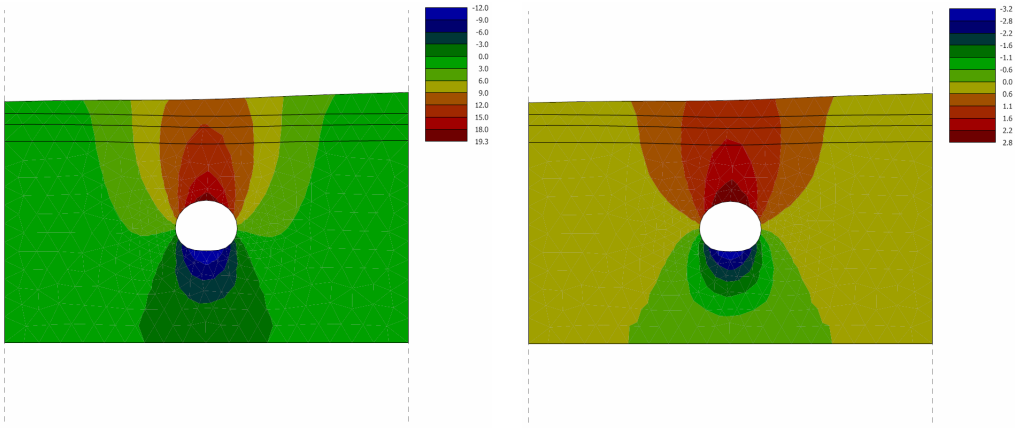

(a) (b)

Figure 5. Vertical displacements: (a) total value before the segment excavation, (b) increment due to the excavation

7. Conclusions

The article provided the theoretical background of the dimensional reduction technique used to simulate the process of continuous tunnel construction in two dimension finite element mesh. The out of plane stiffness and excavation forces are calibrated through in situ measurements of convergence curves. The properties of these curves also allow to refine the possible inaccurate initial stress field. The method was tested on simple elastic excavation problem and the results are comparable with results from the standard convergence confinement method.

Acknowledgment

The support provided by project no. 1M0579 within activities of the CIDEAS research center is gratefully acknowledged.

8. References

Bittnar, Z., Šejnoha J. 1996. *Numerical methods in structural engineering*, ASCE Press and Thomas Telford Publ.

Potts, D. M., Zdravkovič, L. 1999. *Finite element analysis in geotechnical engineering – application*, Thomas Telford, London.

Gramblička, M., Šejnoha, M., Pruška, J. 2004. The use of program GEO FEM for numerical modelling of tunnel Turecký vrch. *Stavební obzor*. Vol. 13(9), 2004:265–271, in Czech.

Barták, J., Macháček J., Pacovský, J 1998. Observation measuring of the earth - covered traffic tunnel structure in the quarry Hvíždalka. *Tunel*. Vol. 7(1), 1998:6–9, in Czech.

Fine Ltd. 2005. GEO FEM - Theory manual, *http://www.fine.cz*.